

---

---

**SHORT  
COMMUNICATIONS**

---

---

## **On the Scenario of Transition to the Broadband Oscillation Regime in the Prototype of a Low-Voltage Vircator**

**Yu. A. Kalinin, A. V. Starodubov\*, and N. N. Kuznetsov**

*Chernyshevsky State University, Astrakhanskaya ul. 83, Saratov, 410012 Russia*

*\*e-mail: StarodubovAV@gmail.com*

Received April 16, 2012

**Abstract**—This study is devoted to experimental investigation of the scenario for a transition from the narrow-band (single-frequency) oscillation regime to the broadband noise-like oscillation in a prototype of a low-voltage oscillator operating with a virtual cathode. The experimental setup and the control instrumentation are considered. Detailed experimental analysis of the dynamics of variation of temporal realizations of the signals generated by the laboratory prototype upon the variation of the chosen control parameters is performed. Analysis of the power spectra, temporal realizations of output signals, phase portraits, and the bifurcation diagram constructed upon a change of the chosen control parameters shows that a transition from the single-frequency oscillation regime to broadband oscillations occurs via a cascade of period-doubling bifurcations (classical Feigenbaum scenario is implemented).

**DOI:** 10.1134/S1063784213060157

### INTRODUCTION

The application of chaotic signals in the systems of data transmission and processing, as well as in the communication system, radiolocation, etc., has attracted considerable attention of researchers in recent years [1–3]. The main advantages of chaotic signals are the wide frequency band ensuring high noise immunity as compared to narrow-band signals and a rapidly decaying autocorrelation function, which makes it possible to use such signals in multiuser communication systems by transmitting several messages in the same frequency range using the code separation of channels as well as easy control over the characteristics.

At present, the microwave range of electromagnetic waves is widely used as the working frequency range in various communication and telecommunication systems. It would be interesting to consider vacuum sources of microwave radiation, which operate as main elements of radiolocation, communication, and telecommunication systems [3]. Such vacuum sources of high-power microwave radiation as oscillators with internal feedback or low-frequency vircators attract considerable attention of researchers because of their significant advantages. First of all, such sources have a simple design and readily tunable oscillation regimes. The operation principle of such devices is based on the formation of the intrinsic electron distributed feedback in a high-intensity electron beam due to the spatial drift of an inhibiting electric field and sometimes a nonuniform magnetic field. The output parameters of such devices were studied earlier in [4–8] theoretically and experimentally, and good agreement between the

theoretical and experimental results was attained. However, in spite of the fact that various oscillation regimes for such devices were considered, it still remains unclear how a transition from one regime to another occurs (in particular, a transition from single-frequency oscillations to broadband oscillations). The solution of this problem will also help to reveal the properties of generated broadband radiation; in particular, it will be clear whether broadband signals being generated belong to chaotic signals (i.e., the Feigenbaum scenario is realized, for example) or to noise signals. Thus, our goal was to study experimentally the scenario of transition from the single-frequency oscillation regime to the regime of broadband oscillations in a laboratory model of a broadband oscillator with intrinsic distributed electron feedback (low-voltage vircator).

### 1. LABORATORY MODEL AND EXPERIMENTAL SETUP

In this study, we consider the scenario of transition from the single-frequency oscillation regime to broadband oscillation regime using the laboratory model of a low-voltage vircator as an example. The photograph of the laboratory prototype is shown in Fig. 1. It is an electronic device with an output power of up to 1 W, operating in the frequency range up to 3 GHz. The intrinsic distributed feedback in such devices is obtained by additional deceleration of the electron flow by applying an inhibiting voltage  $U_{\text{inh}}$  to the collector ( $U_{\text{inh}} < U_0$ , where  $U_0$  is the accelerating voltage). Therefore, an electric field decelerating the electron beam injected from the cathode is produced in the

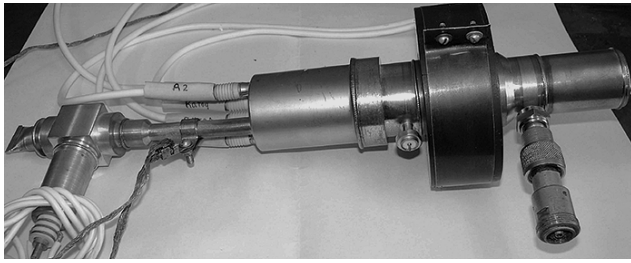


Fig. 1. Photograph of the prototype of the generator of broadband noise-like radiation.

drift space. The power is supplied to the experimental sample of the oscillator in the continuous regime. The main control parameters were accelerating voltage  $U_0$  and voltage  $U_{inh}$  across the collector. The observation and analysis of the dynamics in the model of the low-voltage vircator were carried out using the power spectra and temporal realizations of the signals being generated. The power spectra of the signal were recorded using the Agilent Technologies ESA-E Series Spectrum Analyzer E4402B (9.1 kHz–3.0 GHz). Temporal realizations of the output microwave signals were registered using the Agilent Technologies Infiniium DSO 81004B digital storage series oscilloscope.

## 2. EXPERIMENTAL

The scenario of a transition from the single-frequency oscillation regime to broadband oscillation regime was studied experimentally as follows. The block diagram of the experimental set is shown in Fig. 2. The output signal from the model of the low-voltage vircator was fed to the input of the digital spectrum analyzer, as well as to the input channel of the high-frequency real-time digital storage oscilloscope through a directional splitter. The accelerating voltage applied to the prototype of the low-voltage vircator was chosen as  $U_0 = 800$  V and did not change in the course of experiments. Then, inhibiting voltage  $U_{inh}$  was changed stepwise from the instant at which the single-frequency oscillation mode was observed ( $U_{inh} \approx 725$  V) to the value at which broadband oscillations appeared ( $U_{inh} \approx 780$  V). For each value of inhibiting voltage  $U_{inh}$ , the power spectrum and the temporal realization of the output signal from the laboratory model of the oscillator were recorded. The temporal realization was digitalized at a frequency of 40 GHz, and the duration of each temporal realization was  $50 \times 10^{-6}$  s.

Using the digitalized temporal realizations of the generated output signals, we constructed the phase portraits of the dynamics of the system under investigation for each value of inhibiting voltage  $U_{inh}$  using the Takens method [9, 10].

The processing of the temporal realizations of the output signals enabled us to construct the bifurcation diagram of variation of the dynamics of the laboratory

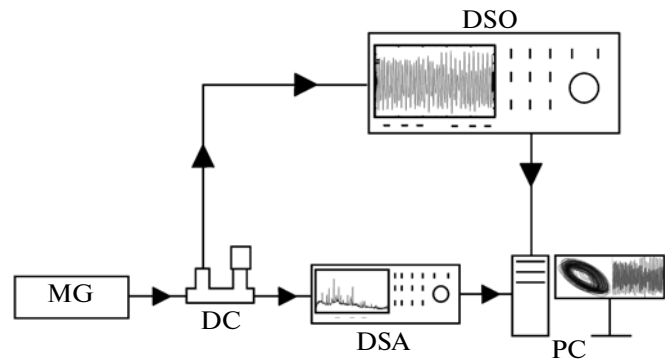
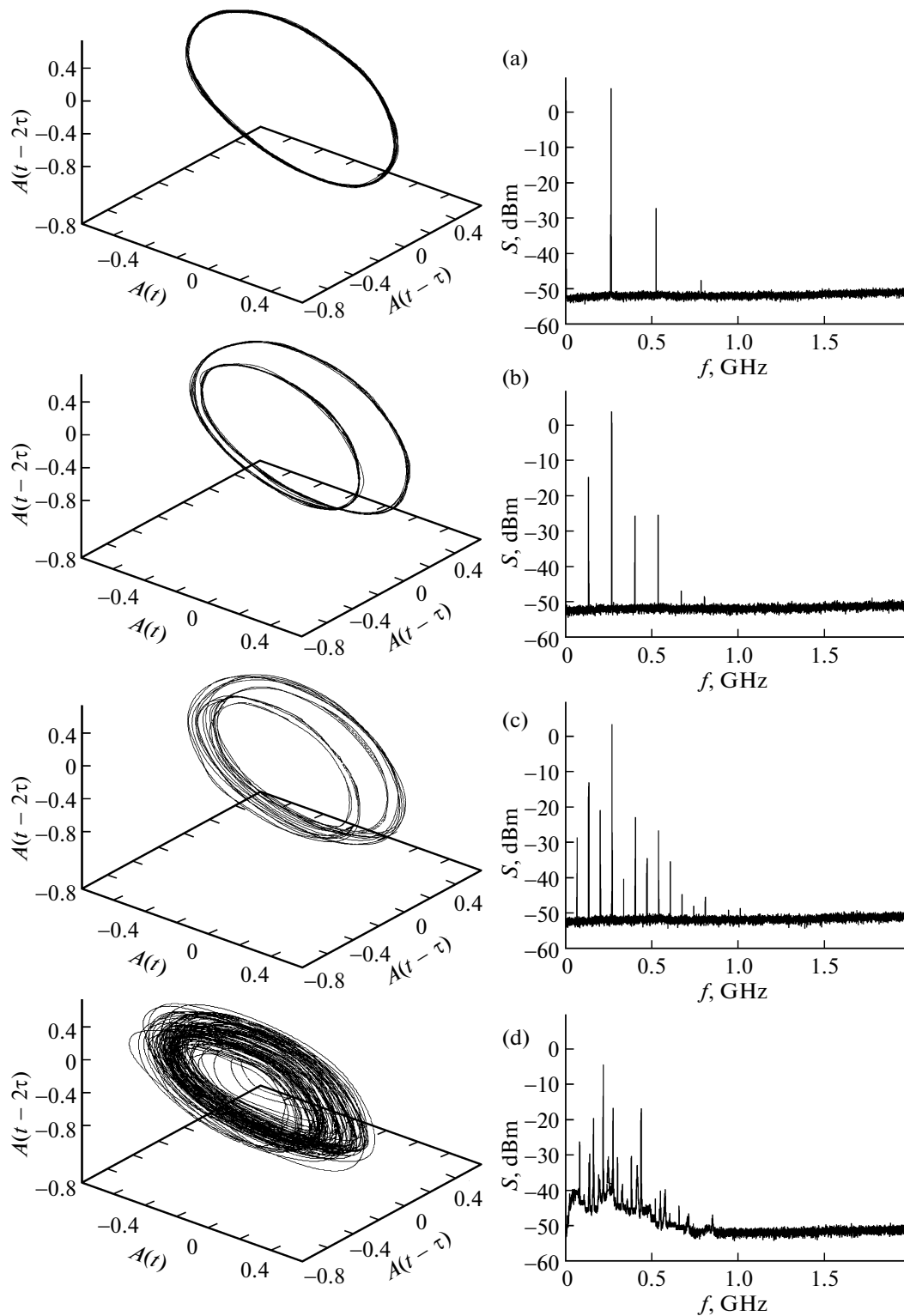


Fig. 2. Block diagram of the experimental setup: microwave generator (MG)—experimental laboratory model of the microwave ultrabroadband oscillator; DC—directional coupler; DSA—digital spectrum analyzer; DSO—digital storage oscilloscope, and PC—personal computer.

prototype of the low-voltage vircator upon a change in inhibiting voltage  $U_{inh}$ . The bifurcation diagram was constructed as follows. In each temporal realization, we searched for local peaks of the time dependence of the output signal amplitude. The resultant array of peak values was plotted on the plane “local peak of signal amplitude  $A$ —voltage  $U_{inh}$  across the collector.” In the case of implementation of the regime of period 1, the time dependence of the output signal amplitude is sinusoidal. The local amplitude peaks in this case are represented by a single value, which is repeated with a certain period. Thus, the dependence of the local amplitude maximum  $A_{max}$  on voltage  $U_{inh}$  across the collector contains only one point for the given value of the accelerating voltage. In the case of realization of the regime of period 2, the temporal realization of the output signal is characterized by two alternating local maxima. Thus, the  $A_{max}(U_{inh})$  dependence now contains two points for the given value of the accelerating voltage. For the cycle of period 4, the temporal realization contains four local maxima alternating with a certain period; accordingly, the  $A_{max}(U_{inh})$  dependence contains four points for the given value of the accelerating voltage. In the case of realization of the broadband oscillation regime, the bifurcation diagram shows that the local maxima of the signal amplitude fill the interval between the minimal and the maximal values of the local maximum for the given value of  $U_{inh}$  almost completely.

## 3. RESULTS

The results of experimental investigations are represented in Figs. 3 and 4. Figure 3 shows the power spectra of the output signal and the phase portraits obtained upon an increase in the inhibiting voltage. It can be seen that with increasing inhibiting voltage, the system under investigation demonstrates a cascade of period doubling bifurcations (i.e., successive emergence of frequencies  $f_0/2$  and  $f_0/4$  in the spectrum of



**Fig. 3.** Results of experimental investigations. Phase portrait (left) and power spectrum (right) obtained for the following values of voltage  $U_{\text{inh}}$  across of the collector: (a) 725; (b) 775; (c)  $\sim 777$ , and (d)  $\sim 790$  V.

the signal, where  $f_0$  is the fundamental frequency of oscillations in the output radiation spectrum of the laboratory prototype of the oscillator). The images of the phase portraits given here also serve as a good illus-

tration of the above results. Unfortunately, analog power supplies used in our experiments did not allow us to observe more than two cascades of period doubling bifurcations.

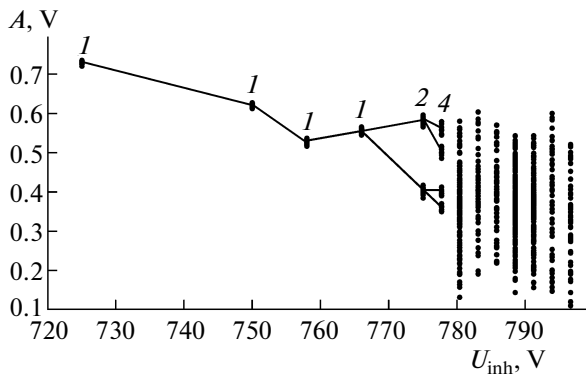


**Fig. 4.** Results of experimental investigations. Bifurcation diagram of the dynamics of variation of the state of the laboratory model of the generator upon an increase in the voltage across the collector: 1—cycle of period 1; 2—cycle of period 2; and 4—cycle of period 4.

Figure 4 shows the bifurcation diagram of the dependence of the dynamics of the laboratory prototype of the low-voltage vircator under investigation on the inhibiting voltage. The bifurcation diagram also clearly illustrates the transition to broadband chaotic oscillations via the cascade of period doubling bifurcations upon an increase in voltage  $U_{inh}$  across the collector.

### CONCLUSIONS

Thus, we have studied experimentally the evolution of the dynamics of a low-voltage vircator from the single-frequency oscillation regime to broadband oscillations upon a change in one of the control parameters (namely, the voltage across the collector). It has been established that for a certain value of the accelerating voltage, a cascade of period doubling bifurcations is realized in the prototype of the low-voltage vircator during the transition to the broadband oscillation regime; in other words, the classical scenario of a transition to chaos (Feigenbaum scenario) is realized. This enables us to state that the broadband oscillation

regime considered here for the given values of the control parameters of the experimental setup is basically chaotic.

### ACKNOWLEDGMENTS

The authors thank A.S. Fokin for assistance.

This work was supported by the Russian Foundation for Basic Research (project nos. 10-02-00256-a and 12-02-90022-Bel\_a).

### REFERENCES

1. N. N. Zalugin and V. V. Kislov, *Wideband Chaotic Signals in Radio Engineering and Information Systems* (Radiotekhnika, Moscow, 2006).
2. A. S. Dmitriev and A. I. Panas, *Dynamical Chaos: New Information Media for Communication Systems* (Fizmatlit, Moscow, 2002).
3. D. I. Trubetskov and A. E. Khramov, *Lectures on Microwave Electronics for Physicists* (Fizmatlit, Moscow, 2003–2004), Vols. 1, 2.
4. *Methods of Nonlinear Dynamics and Chaos in Problems of Microwave Electronics*, Vol. 2: *Nonstationary and Chaotic Processes*, Ed. by D. I. Trubetskov, A. A. Koronovskii, and A. E. Hramov (Fizmatlit, Moscow, 2009).
5. Yu. A. Kalinin, S. A. Kurkin, D. I. Trubetskov, and A. E. Khramov, *Usp. Sovr. Radioelektron.*, No. 9, 53 (2008).
6. Yu. A. Kalinin and A. V. Starodubov, "Perspective superbroadband chaos generators on high and super-high frequency," *Kratk. Soobshch. Fiz.* **37** (5), 3 (2010).
7. E. N. Egorov, Yu. A. Kalinin, A. A. Koronovskii, and A. E. Khramov, *Tech. Phys.* **52**, 1387 (2007).
8. E. N. Egorov, Yu. A. Kalinin, A. A. Koronovskii, Yu. I. Levin, and A. E. Khramov, *Radiotekh. Elektron.* **52**, 51 (2007).
9. F. Takens, *Dynamical Systems and Turbulence*, Ed. by D. Rand and L.-S. Young (Springer, Berlin, 1981), p. 366.
10. S. P. Kuznetsov, *Dynamic Chaos* (Fizmatlit, Moscow, 2001).

*Translated by N.V. Wadhwa*